

原著

# Investigation of converter for assuring beam component fluence distribution by imaging plate in boron neutron capture therapy—Combination with gamma-ray shield to detect fast neutrons

Kenichi Tanaka<sup>1\*</sup>, Tsuyoshi Kajimoto<sup>2</sup>, Yoshinori Sakurai<sup>3</sup>, Takushi Takata<sup>3</sup>, Hiroki Tanaka<sup>3</sup>, Gerard Bengua<sup>4</sup>, Satoru Endo<sup>2</sup>

<sup>1</sup>Laboratory of Physics, Kyoto Pharmaceutical University

<sup>2</sup>Advanced Science and Engineering, Hiroshima University

<sup>3</sup>Institute for Integrated Radiation and Nuclear Science, Kyoto University

<sup>4</sup>Auckland City Hospital

The spatial distributions of neutrons and gamma rays in a boron neutron capture therapy (BNCT) irradiation field should be measured separately as the quality assurance. For this purpose, the present study investigated the advantage of using a beam component shield and beam component-enhancing converter together with an imaging plate. The suitable configurations of the shield and converter were surveyed through simulations using PHITS (Particle and heavy ion transport code system). The BNCT irradiation field used in the simulations was assumed to have been generated via the  ${}^7\text{Li(p,n)}$  reaction at an incident proton energy of 2.5 MeV, where neutrons were moderated with 200-mm-thick  $\text{D}_2\text{O}$ . Several potentially usable converters were found for a 60-mm-thick bismuth gamma-ray shield.

Keywords: BNCT, Quality assurance, Imaging plate, Beam component

受付日：2024年5月29日，受理日：2024年6月18日

## 1. Introduction

The quality assurance (QA) of the spatial distribution of the beam intensity in boron neutron capture therapy (BNCT) requires the detection systems to

measure the distributions of neutrons and gamma rays<sup>1)</sup>. Ideally, the system should be able to separately measure the neutron components of the irradiation field based on the neutron energy, i.e., thermal ( $-0.5$  eV), epithermal ( $0.5$  eV– $10$  keV), and fast neutrons ( $10$  keV–).

The imaging plate (IP) is a handy and commercially available tool to measure the two-dimensional distribution of radiation intensity<sup>2–4)</sup>. We have been developing a method to determine two-dimensional

\* 連絡先：  
Laboratory of Physics, Kyoto Pharmaceutical University  
5 Misasaginakauchi-cho, Yamashina-ku, Kyoto 607-8414, Japan

spatial distribution of the beam component fluence using the IP<sup>5,6)</sup>. In these works, it is not the absolute value of the fluence but its relative distribution that should be estimated for the purpose of a QA of the beam profile. As reported by Nakamura and Inabe<sup>7)</sup> and Boukhair et al.<sup>8)</sup>, the IP has the sensitivity for neutrons at one to two orders of magnitude lower than that for gamma rays. Reflecting this feature, the simulation calculation<sup>5)</sup> and experimental verification using a clinical BNCT beam<sup>6)</sup> indicated that it was difficult to measure the fast neutron component because the signal intensity of the IP for gamma rays was much higher than that for fast neutrons. In these studies, it was attempted to enhance the sensitivity of the IP to fast neutrons by using the recoil protons from the hydrogen-rich material. As an option to overcome this, the present study attempts to decrease gamma rays by using a gamma-ray shield, and to relatively increase the fast neutron contribution to the signal intensity of the IP.

## 2. Materials and methods

This study was performed with the simulation

calculations using PHITS (version 2.82)<sup>9)</sup>.

### 2.1 Simulation of irradiation field

The irradiation field in the calculations was detailed in previously<sup>5)</sup>, and the usability of this field in BNCT was demonstrated based on the dose required for BNCT treatment<sup>10)</sup>. The geometry of beam shaping assembly is shown in **Fig. 1**. The geometry consists of a Li target of 100 mm in diameter and 3 mm in thickness, a D<sub>2</sub>O moderator of 200 mm in thickness and diameter, and a collimator made of the mixture of polyethylene and natural LiF with 50 wt%. The beam components of neutrons and gamma ray at the aperture of the collimator were calculated by transporting neutrons and gamma rays from the target bombarded with 2.5 MeV protons. The fluence of irradiation fields was  $3.53 \times 10^7$  for thermal neutron,  $1.33 \times 10^8$  for epithermal neutron,  $7.99 \times 10^7$  for fast neutron, and  $9.96 \times 10^7$  particle/cm<sup>2</sup>/mC for gamma ray. In this simulation, sourced neutrons and gamma rays were generated from the aperture of the collimator and were transported in a detector consisting of IP, converter, and gamma-ray shield.

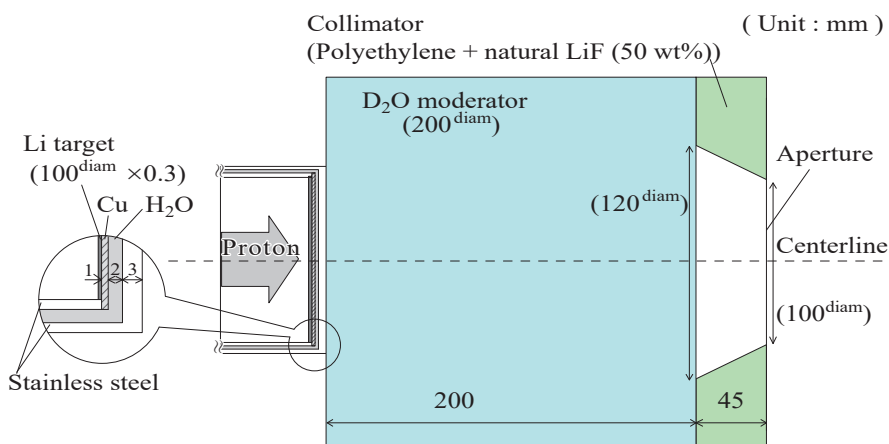


**Fig. 1** Cross-sectional configuration of beam shaping assembly.

## 2.2 Imaging plate, converter, and gamma-ray shield

The instrument for the QA of the spatial distribution of the beam component fluence assumed in this study consisted of an IP, converter, and gamma-ray shield. The calculation geometry is shown in Fig. 2. The geometry does not include the Li target, moderator, or collimator. Instead, as a simulation of the geometry where the IP, converter, and gamma-ray shield are placed at the aperture of the collimator, one side of the gamma-ray shield was set as a plane source of neutrons and gamma rays. Among the neutrons and gamma rays in Fig. 1, each of four beam components, i.e., thermal neutrons, epithermal neutrons, fast neutrons, and gamma rays, was produced in calculation separately in order to simulate the irradiation by each of the incident beam component. The angular distribution of the source particles (neutrons and photons) were set similarly to the previous calculation that tallied those particles at collimator aperture in Fig. 1.

The IP modeled in the simulations was the “BAS-TR,” which is manufactured by Fuji Film Corporation, Japan. The BAS-TR IP consists of a detector layer (thickness: 50  $\mu\text{m}$ ) made of  $\text{BaF}(\text{Br}_{0.85}\text{I}_{0.15})\text{:Eu}$ , and two support layers (thicknesses: 250  $\mu\text{m}$  and 160  $\mu\text{m}$ ) made of polyethylene terephthalate and  $\text{FeOMn}_{0.189}$ , in turn. The detector layer, which

records the amount of the energy deposited by the radiation, is not covered with the packing material, accordingly the secondary charged particles from the converter such as electron, proton, alpha particle, and  $^7\text{Li}$  ion reach the detector layer and deposit the energy. Nuclear data libraries—JENDL-4 (Japanese evaluated nuclear data library)<sup>(11)</sup> for neutron transport and EPDL97 (Evaluated photon data library, 1997 version)<sup>(12)</sup> for gamma ray transport were used in the calculation.

In the calculation using the PHITS code in the present study, the IP dimensions were set at  $20 \times 20 \text{ mm}^2$  and the IP was surrounded by the converter and gamma-ray shield. Various thicknesses of the gamma-ray shield were examined. The event generator mode<sup>(13)</sup> was applied. The energy deposition at the detector layer of the IP was computed using the “T-deposit tally” in dose mode. The energy deposited by all kinds of particles for each of the incident beam components, i.e., thermal, epithermal, fast neutrons, and gamma rays, was treated as a representation of the IP signal for the irradiation of the beam component. The converter materials considered were as follows: (1) epoxy resin ( $\text{C}_{28}\text{H}_{32}\text{O}_6$ ) to enhance the sensitivity of IP to the fast neutrons via recoil protons, (2) epoxy resin doped with  $^{10}\text{B}$  to enhance that to thermal and epithermal neutrons via secondary particles from the  $^{10}\text{B}(\text{n},\alpha)^7\text{Li}$  reaction, and (3) graphite to enhance that to the gamma-rays. Graphite is not expected to enhance the neutrons, because of its low neutron interaction cross-section, but it will enhance the sensitivity of the IP to gamma rays via the secondary electrons. The resin for thermal and epithermal neutrons was a  $\text{B}_4\text{C}/\text{epoxy}$  composite, where the boron is enriched with  $^{10}\text{B}$  at a concentration of 100%. For the gamma-ray shield, Bi was used because of its low yield of secondary gamma rays during neutron irradiation compared

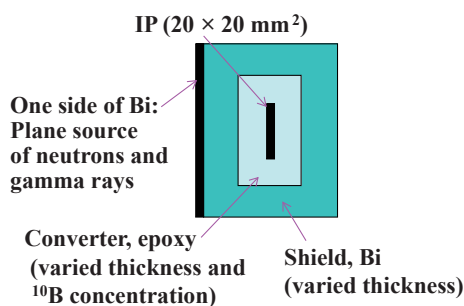


Fig. 2 Calculation geometry.

with conventional gamma-ray shields such as Pb.

### 2.3 Method to estimate beam component fluence

The present investigation was performed assuming two styles of fluence estimation. In the first method, the fluence of four beam components was to be estimated using the results of the measurements for four IPs. This method is briefly described here; the details have been discussed in a previous paper<sup>6)</sup>. The beam component fluence  $\phi_j$  of the beam component  $j$  can be estimated using Eqs. (1) and (2):

$$PSL = \begin{pmatrix} PSL_1 \\ PSL_2 \\ PSL_3 \\ PSL_4 \end{pmatrix} = \begin{pmatrix} a_{11} & a_{12} & a_{13} & a_{14} \\ a_{21} & a_{22} & a_{23} & a_{24} \\ a_{31} & a_{32} & a_{33} & a_{34} \\ a_{41} & a_{42} & a_{43} & a_{44} \end{pmatrix} \begin{pmatrix} \phi_1 \\ \phi_2 \\ \phi_3 \\ \phi_4 \end{pmatrix} = A \cdot \phi, \quad (1)$$

$$\phi = A^{-1} \cdot PSL. \quad (2)$$

Here, photostimulated luminescence (*PSL*) denotes the IP signal intensity, which can be obtained from the measurements. The subscript  $i$  identifies the configuration of the converter and gamma-ray shield which contains the IP while  $a_{ij}$  denotes the sensitivity of the  $i$ th configuration around the IP for the beam component  $j$ . The energy deposition at the detector layer of the IP per unit particle fluence computed from the PHITS simulations is considered to represent its sensitivity.

In the second method, the fluence of one beam component was to be estimated by simply subtracting the IP signal intensities between two configurations. This is based on the idea that the estimation combining the results of more IPs produces larger error because the result for each IP has an error.

### 2.4 Selection of converter and gamma-ray shield

Suitable dimensions of the converters and shield were investigated for the usage of two methods to estimate the beam component fluence. In addition, the suitable  $^{10}\text{B}$  concentrations in the epoxy were

also surveyed for the converter for thermal and epithermal neutrons. The calculation was performed for 0–10 mm of converter thickness, 0–80 mm of shield thickness, and 0–50% of  $^{10}\text{B}$  concentration. The converter and shield were chosen such that the contribution of the attempted beam component to the energy deposition on the IP was over 21%. This is based on the previous study<sup>6)</sup> which suggested that the beam component providing an energy deposition on the IP of 21% or more of the total would be successfully estimated.

### 2.5 Distortion of beam component by gamma-ray shield

For gamma-ray shields as thick as several centimeters, there is a concern that the initial shape of the distribution of the beam component fluence may totally disappear due to the distortion of the irradiation field by the shield. Thus, it was attempted to confirm how much distortion from the initial beam component distribution was caused by the presence of a gamma-ray shield and IP. This was carried out by calculating the shape of the fluence distribution at the beam edge at the detector layer of the IP placed in the gamma-ray shield. In order to check the beam edge clearly, the simulation in this case was performed for an imaginary parallel beam. The radius of the beam, i.e., the source of the neutrons and gamma rays on Bi surface was set to 5 mm, as an example. The Bi thickness was set as chosen in the investigation in Sec. 2.4. The radial distribution of the fluence in the sensitive region of the IP without the converter was tallied at 1-mm increments.

### 3. Results and discussion

#### 3.1 Selection of gamma-ray shield thickness

The relation between energy depositions on the IP and Bi thickness is presented in **Fig. 3**. The converter, in this case, is epoxy resin with a thickness of 1 mm, which was found to be potentially usable for enhancing the fast neutron component<sup>5)</sup>. From **Fig. 3(a)**, the energy deposited by gamma rays decreased by about one order of magnitude for the Bi thickness of about 40 mm. The energy deposited by neutron components was almost constant for fast neutrons and slightly increased for thermal and epithermal neutrons due to moderation of higher energy components. This aspect influences the required and acceptable duration time of the QA irradiation using the IP proposed in the present study. The previous test<sup>6)</sup> using the clinical BNCT beam at the Kyoto University Reactor<sup>14)</sup> suggested that the signal intensity of the IP reached its saturation by 4 minutes of irradiation. The IP has a dynamic range of five orders of magnitude<sup>15)</sup>; therefore, even if a Bi thick-

ness of tens of millimeters is used as the gamma-ray shield, the QA irradiation can be performed in a reasonable time of several minutes.

The beam component contribution to the total energy deposition on the IP is shown in **Fig. 3(b)**. As the Bi thickness increased, the contribution from gamma rays decreased and those from the neutron components increased. The configuration consisting of Bi with a thickness of 60 mm was investigated further at the following sections, because that yielded comparable contribution of neutrons and gamma rays.

#### 3.2 Distortion of spatial distribution of beam component by gamma-ray shield

The radial distribution of the beam component fluence in the detector layer of the IP without the converter is shown in **Fig. 4**. The distribution is normalized to unity at the center of the IP, i.e., at the radial distance of 0–1 mm. The fluence distribution was uniform within 5% in the region up to 5 mm in radius, where the uniform beam is incident. Compared to this, the decrease in the fluence near the beam edge will be because the beam is not impinged

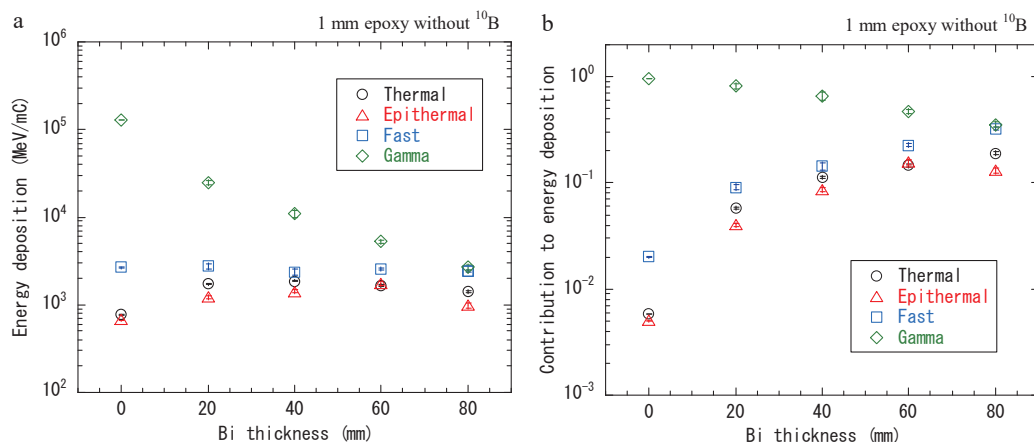


**Fig. 3** Dependence of (a) energy deposition on IP in 1-mm-thick epoxy resin; and (b) contribution from beam component on Bi thickness.

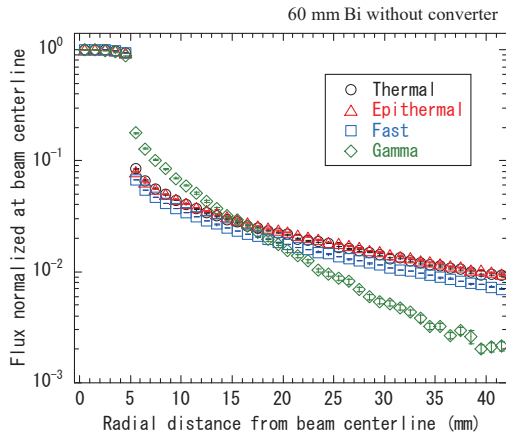


**Fig. 4** Radial distribution of fluence component on IP in 60-mm-thick Bi for parallel incident beam of 5 mm in radius.

over 5 mm in radius, which decreases the particles scattered outside the beam edge and delivered to the region within 5 mm in radius. The fluence at the region with a radius of 5–6 mm, which was directly adjacent to the edge of the beam, is 6–9% for neutrons and 18% for gamma rays. The fluence decreased to a few percents of the incident fluence at a radial distance of about 20–40 mm. This is the characteristic distortion by the 60-mm-thick Bi, chosen in Sec. 3.1. In addition, the converters will cause further distortion. When the initial beam shape without distortion is required, the measured values should be further analyzed by deconvolution for example. On the other hand, the present study focuses on the QA of the beam component distribution, which will enable the detection of temporal changes in the distribution. In this case, the distribution without the distortion is not always required, while it is desirable to estimate without distortion if possible. However, as long as the IP is sensitive to the beam component of interest at an acceptable level, the distorted distribution can still be used for the purpose of QA. Thus, the distortion does not instantly prohibit the use of the proposed method.

This discussion is also applicable to the distortion of the energy spectrum, angular distribution, etc. Another issue for the QA process is how small decrease in the component intensity can be detected. As to the usability, the experimental verification is recommended because there may be the cases where the change in the fluence distribution is compensated by the distortion and cannot be detected.

### 3.3 Selection of converter configuration for component separation in gamma-ray shield

The dependences of (a) the energy deposition in the IP and (b) its contribution by the beam component on  $^{10}\text{B}$  concentration in the epoxy resin are shown in **Fig. 5**. The gamma-ray shield used here was the 60-mm-thick Bi as chosen in Sec. 3.1. The thickness of the epoxy resin was 1 mm as a candidate<sup>5)</sup>. For the epoxy resin without  $^{10}\text{B}$ , i.e., at a  $^{10}\text{B}$  concentration of 0%, the contribution from fast neutrons was 23%, which satisfies the attempted value over 21%. For higher  $^{10}\text{B}$  concentrations, the other neutron components are expected to be measured separately, e.g., thermal neutrons with a contribution of 62% at the  $^{10}\text{B}$  concentration of 1%, and epithermal neutrons with a contribution of 58% at the  $^{10}\text{B}$  concentration of 10%.

The dependence of the energy deposition on the thickness of the epoxy resin with 10%  $^{10}\text{B}$  is shown in **Fig. 6**. As the thickness increased over 1 mm, the contribution from epithermal neutrons became dominant. The thickness should be chosen so that the beam component of interest has attempted value of contribution to total energy deposition.

The candidate converter configurations are listed in **Table 1** for the fluence estimation using the results of four IPs. The values listed in **Table 1** are the contribution from the beam component to the total of the energy deposition, such as the values in

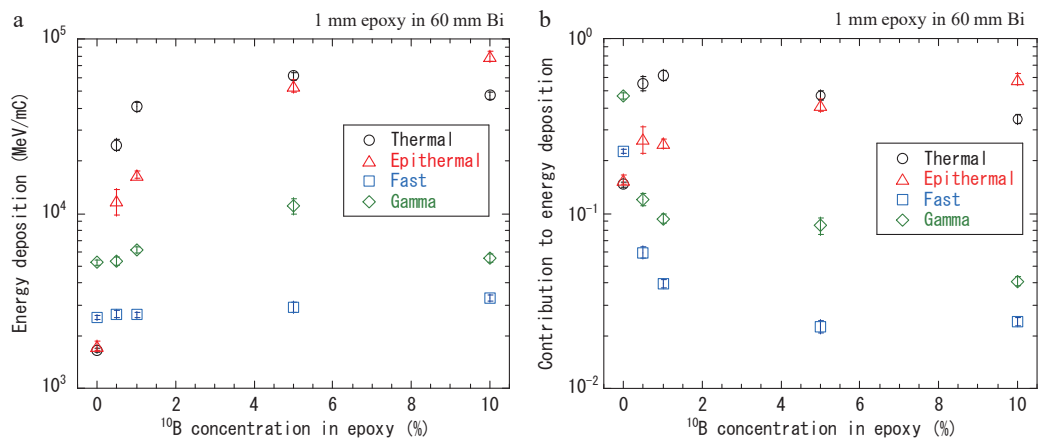


Fig. 5 (a) Energy deposition on IP; and (b) its beam component contribution dependent on  $^{10}\text{B}$  concentration in geometry with 60-mm-thick Bi.

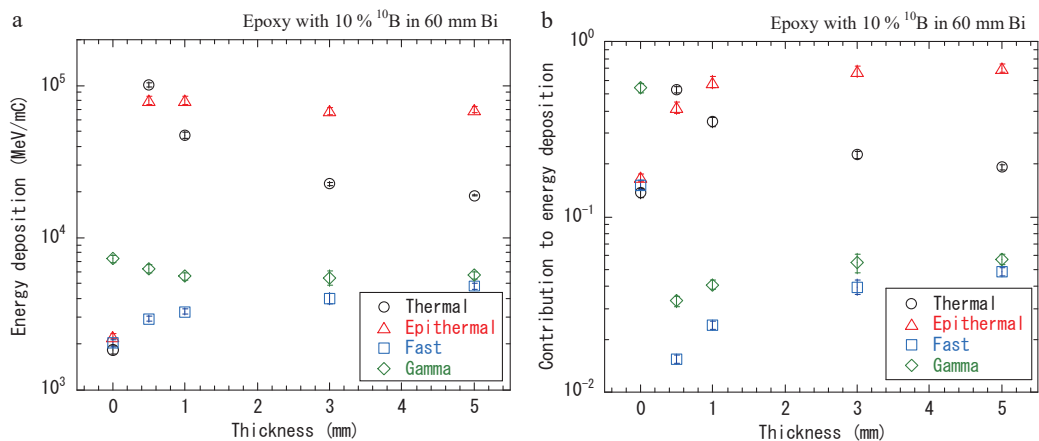


Fig. 6 Dependence of (a) energy deposition; and (b) its beam component contribution on epoxy resin thickness with 10%  $^{10}\text{B}$  in 60-mm-thick Bi.

Table 1 Contribution (%) from beam component to energy deposition on IP for the fluence estimation using the results of four IPs.

The underlined numbers indicate the contributions from the components we attempted to detect.

Converter configuration	With 60 mm thick Bi				Without Bi			
	Thermal	Epi	Fast	Gamma	Thermal	Epi	Fast	Gamma
1 mm Epoxy with 1% $^{10}\text{B}$	<u>62</u>	25	4	9	<u>26</u>	7	1	66
1 mm Epoxy with 10% $^{10}\text{B}$	35	<u>59</u>	2	4	28	<u>27</u>	1	45
1 mm Epoxy with 50% $^{10}\text{B}$	18	<u>76</u>	3	3	11	<u>48</u>	1	40
5 mm Epoxy with 10% $^{10}\text{B}$	19	<u>70</u>	5	6	6	<u>32</u>	2	60
1 mm Epoxy without $^{10}\text{B}$	15	16	<u>23</u>	47	0.5	0.5	<u>2</u>	97
1 mm Graphite	12	11	21	<u>55</u>	0.4	0.6	1	<u>98</u>
No Converter	14	17	15	<u>54</u>	0.3	0.5	1.7	<u>97.5</u>

**Figs. 3(b), 5(b) and 6(b).** The configuration of “No Converter” corresponds to the converter thickness of 0 mm in **Figs. 6**. For comparison, the results for the corresponding geometry without Bi are also listed<sup>5)</sup>. The use of the gamma-ray shield has the advantage of increasing the contribution from neutron components by decreasing the contribution from gamma rays. Specifically, the fast neutron contribution significantly improved by including Bi, i.e., from 2 to 23%, and is therefore expected to be detected successfully. A simple configuration would be 1-mm-thick converters made of epoxy resin combined with 1%  $^{10}\text{B}$  for thermal neutrons, 50%  $^{10}\text{B}$  for epithermal neutrons, 0%  $^{10}\text{B}$  for fast neutrons, and a graphite converter or no converter for gamma rays.

Here, the relationship between the IP signal and the energy deposition in the detector layer of the IP is dependent on the type of the particle which enhances the interested beam component. Thermal neutrons, epithermal neutrons, fast neutrons, and gamma rays deposit energy via alpha particles and  $^7\text{Li}$  nuclei from the  $^{10}\text{B}(\text{n},\alpha)^7\text{Li}$  reaction, alpha particles and  $^7\text{Li}$  nuclei, recoil protons, and secondary electrons, respectively. Recoil protons and secondary electrons deposits the energy all through the 50- $\mu\text{m}$ -thick detector layer of the IP, while the energy deposition depends on the depth from the surface. However, alpha particles and  $^7\text{Li}$  nuclei have ranges of several micrometers. Though the details were discussed previously<sup>5)</sup>, the energy deposition to be the IP signal is expected to be lower for recoil protons and secondary electrons than alpha particles and  $^7\text{Li}$  nuclei, by possibly tens of percentages<sup>4, 16)</sup>. This is because attenuation of the photoluminescence to be detected by the IP reader reduces the efficiency. Also, because of signal fading, the IP signal produced by alpha particles reduces more rapidly than those by X-rays by 30–40%<sup>7)</sup>. These factors have

opposite influences. In total, the type of radiation could double contribution of a certain beam component to the total of the IP signal at most. This effect is included by doubling the energy deposition from one or more of the beam components. Considering this, the design goal of the energy deposition contribution in Sec. 2.4 is 12% by doubling thermal and epithermal contributions. In this case, the aforementioned simple configuration of the converter in **Table 1** still has the energy deposition contributions over the design goal, e.g. at least 17% for fast neutrons for 1 mm epoxy without  $^{10}\text{B}$ . By combining the gamma-ray shield with the converter with higher hydrogen composition such as polyethylene, the fast neutron contribution will possibly be increased further.

For the fluence estimation by the subtraction between two IP signal intensities, it is desirable that only one beam component has different values of the energy deposition on the two IPs while the other components have identical values. This condition is observed in **Fig. 5(a)**, where the energy deposition by epithermal neutrons changed more significantly than those from the other components for  $^{10}\text{B}$  concentrations between 1 and 10%. In addition, in **Fig. 6(a)**, the energy deposition by thermal neutrons changed between the thicknesses of 0.5 and 1 mm.

The potential converter combinations with the 60-mm-thick Bi are listed in **Table 2** together with the contribution from the component to the energy deposition on the IP. Here, the configuration “A–B” indicates that the energy deposition for converter “B” is subtracted from that for “A.” When the contribution from unattempted components up to 1% is accepted, configuration #1, which corresponds to “epoxy with 10%  $^{10}\text{B}$  of <0.5–1 mm> thickness,” is usable in the thermal neutron measurement. If 10% of the energy deposition contribution from the unat-



tempted component is accepted, configuration #2, which corresponds to “epoxy with 10%  $^{10}\text{B}$  of <0.5–5 mm> thickness,” is applicable to thermal neutron measurements, and configuration #3 is the “1-mm epoxy with <10–1%>  $^{10}\text{B}$ ” to epithermal neutrons. The combination with the energy deposition dominated by fast neutrons was not found. However, in configuration #4 (“1 mm <Epoxy without  $^{10}\text{B}$ –Graphite>”), the fast neutron contribution was 28%, which satisfies the design goal of 21% shown in Sec. 2.4. For detection of gamma rays, the configurations #5 “<No Converter–1 mm Graphite>” and #6 “<1 mm Graphite–0.1 mm Epoxy without  $^{10}\text{B}$ >” have sufficiently high contribution of 52% and 56%, respectively. For this, the potential combination is #1, #3, #4, and #5. Even if the relationship between the IP signal and the energy deposition dependence on the particle type is considered, the energy deposition contributions are still over the design goal, e.g. at least 18% for fast neutrons for #4, while the design goal is changed to 12% by this consideration. In this case, six IPs are required as some of the configurations use the same converter. From the viewpoint of reducing the number of IPs for the sake of handiness, the estimation using four IPs chosen from the configurations listed in **Table 1** is better for the fast neutron component. However, if the distortion of the component distribution is at the acceptable level,

the subtraction will also be potentially usable in thermal and epithermal neutron estimations in configurations #1, #2, and #3.

## 4. Conclusion

The usability of the converter and gamma-ray shield combined with IP to measure the BNCT beam components has been investigated by simulations using PHITS for an irradiation field generated from  $^7\text{Li}(p,n)$  neutrons at an incident proton energy of 2.5 MeV, where neutrons are moderated with 200-mm-thick  $\text{D}_2\text{O}$ . For a 60-mm-thick Bi gamma-ray shield, potentially usable converters were found. In this case, the fast neutron fluence estimation by the sensitivity matrix of the IPs in four configurations is more promising from the viewpoint of handiness, compared with the estimation by simply subtracting the IP signal intensities between two configurations. This study has demonstrated the advantage and basic idea of combining the converter and shield in the QA of the beam component distribution.

## [Acknowledgement]

This work was supported by JSPS KAKENHI Grant Numbers 23K07118, 20K08050, JP26293281, and

**Table 2** Potential converter combinations in 60-mm-thick Bi for the fluence estimation by the subtraction of two IP signal intensities.

The configuration “A–B” indicates that the energy deposition for converter “A” is subtracted from that for “B.”

#	Converter configuration	Thermal	Epi	Fast	Gamma
1	Epoxy with 10% $^{10}\text{B}$ of <0.5–1 mm> thickness	<u>99</u>	0	–1	2
2	Epoxy with 10% $^{10}\text{B}$ <0.5–5 mm> thickness	<u>90</u>	11	–2	1
3	1 mm Epoxy with <10–1%> $^{10}\text{B}$	9	<u>91</u>	1	–1
4	1 mm <Epoxy without $^{10}\text{B}$ –Graphite>	24	31	<u>28</u>	17
5	<No Converter–1 mm Graphite>	17	27	4	<u>52</u>
6	<1 mm Graphite–0.1 mm Epoxy without $^{10}\text{B}$ >	14	14	16	<u>56</u>

JP24659568. This work was partially supported by the Joint Usage/Research of the Institute for Integrated Radiation and Nuclear Science, Kyoto University (KURNS). The authors express their sincere appreciation to Mr. Seisuke Noguchi in Innovation Plaza of Hiroshima University and Mr. Yoshiyuki Kanazawa in the workshop at Sapporo Medical University, Japan for their support in the investigations.

#### [Ethics approval and consent to participate]

There is nothing to declare.

#### [Conflict of Interest]

The authors declare no conflict of interest

#### [Reference]

- 1) International Atomic Energy Agency (IAEA). *Current status of neutron capture therapy*. IAEA-TECDOC-1223, **2001**, IAEA, Vienna, Austria.
- 2) Yutaka Amemiya, Jun Miyahara. Imaging plate illuminates many fields. *Nature* **1988**, 336, 89–90.
- 3) Kenji Takahashi, Seiji Tazaki, Junji Miyahara, Yuuko Karasawa, Nobuo Niimura. Imaging performance of imaging plate neutron detectors. *Nucl. Inst. Meth. Phys. Res.* **1996**, A377, 119–122.
- 4) Michael Thoms. The quantum efficiency of radiographic imaging with image plates. *Nucl. Inst. Meth. Phys. Res.* **1996**, A378, 598–611.
- 5) Kenichi Tanaka, Yoshinori Sakurai, Satoru Endo, Jun Takada. Study on detecting spatial distribution of neutrons and gamma rays using a multi-imaging plate system. *Appl. Rad. Isot.* **2014**, 88, 143–146.
- 6) Kenichi Tanaka, Yoshinori Sakurai, Hiroki Tanaka, Tsuyoshi Kajimoto, Takushi Takata, Jun Takada, Satoru Endo. Measurement of spatial distribution of neutrons and gamma rays for BNCT using multi imaging plate system. *Appl. Rad. Isot.* **2015**, 106, 125–128.
- 7) Shoji Nakamura, Ken Inabe. Response and fading behavior of an imaging plate to  $\alpha$ ,  $\beta$ , and  $\gamma$  rays. *Radiation* **1999**, 2, 25–30.
- 8) Artu Boukhaïr, Creg Heilmann, Auri Nourreddine, Ares Pape, Greg Portal. Fast neutron and  $\gamma$ -ray dosimetry with imaging plates. *Rad. Meas.* **2001**, 34, 513–516.
- 9) Tatsuhiko Sato, Koji Niita, Norihiro Matsuda, Shintaro Hashimoto, Yosuke Iwamoto, Shusaku Noda, Tatsuhiko Ogawa, Hiroshi Iwase, Hiroshi Nakashima, Tokio Fukahori, Keisuke Okumura, Tetsuya Kai, Satoshi Chiba, Takuya Furuta, Lembit Sihver. Particle and heavy ion transport code system PHITS, Version 2.52. *J. Nucl., Sci. Technol.* **2013**, 50, 913–923.
- 10) Kenichi Tanaka, Tooru Kobayashi, Gerard Bengua, Yoshinobu Nakagawa, Satoru Endo, Masaharu Hoshi. Characterization of moderator assembly dimension for accelerator boron neutron capture therapy of brain tumors using  ${}^7\text{Li}(p,n)$  neutrons at proton energy of 2.5 MeV. *Med. Phys.* **2006**, 33, 1688–1694.
- 11) Keiichi Shibata, Osamu Iwamoto, Tsuneo Nakagawa, Nobuyuki Iwamoto, Akira Ichihara, Satoshi Kunieda, Satoshi Chiba, Kazuyoshi Furutaka, Naohiko Otuka, Takaaki Ohsawa, Toru Murata, Hiroyuki Matsunobu, Atsushi Zukeran, So Kamada, Jun-ichi Katakura. JENDL-4.0: A new library for nuclear science and engineering. *J. Nucl. Sci. Technol.* **2011**, 48(1) 1–30.
- 12) Dermott Cullen, John Hubbell, Lynn Kissel. EPDL97: the evaluated photon data library, '97 version. *UCRL--50400*, **1997**, 6(5) 1–33.
- 13) Yosuke Iwamoto, Koji Niita, Tatsuhiko Sato, Norihiro Matsuda, Hiroshi Iwase, Hiroshi Nakashima, Yukio Sakamoto. Application and validation of event generator in the PHITS code for the low-energy neutron-induced reactions. *Prog. Nucl. Sci. Technol.* **2011**, 2, 931–935.
- 14) Yoshinori Sakurai, Tooru Kobayashi. Characteristics of the KUR Heavy Water Neutron Irradiation Facility as a neutron irradiation field with variable energy spectra. *Nucl. Instr. Meth.* **2000**, A453, 569–596.
- 15) Michael Thoms. Neutron detection with imaging plates Part II. Detector characteristics. *Nucl. Inst. Meth. Phys. Res.* **1999**, A424, 34–39.
- 16) Thopus Bonnet, Michael Comet, Denis Petit, Fourde Gobet, Frues Hannachi, Mores Tarisien, Miche Versteegen, Marie Aleonard. Response functions of Fuji imaging plates to monoenergetic protons in the energy range 0.6–3.2 MeV. *Rev. Sci. Instr.* **2013**, 84, 013508.